

Coexistence of Ion Pairs and Charge-Transfer Complexes and Their Impact on Pentacene Singlet Fission

Christoph P. Theurer, Martin Richter, Debkumar Rana, Giuliano Duva, Daniel Lepple, Alexander Hinderhofer, Frank Schreiber, Petra Tegeeder,* and Katharina Broch*

Cite This: *J. Phys. Chem. C* 2021, 125, 23952–23959

Read Online

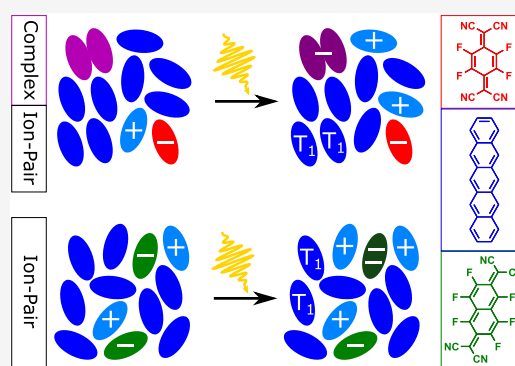
ACCESS |

Metrics & More

Article Recommendations

Supporting Information

ABSTRACT: Pentacene (PEN) is a prototypical small-molecule organic semiconductor and a singlet fission (SF) material, but the details of its charge-transfer (CT) interactions with electron acceptors are still under debate. Here, we revisit the CT interactions in thin film blends of PEN and 2,3,5,6-tetrafluoro-7,7,8,8-tetracyanoquinodimethane (F4-TCNQ) and find experimental evidence for the coexistence of integer CT (ICT) and charge-transfer complex (CTC) formation, with the relative amount depending on the mixing ratio. In contrast, in blends of PEN and 2,2'-(perfluoronaphthalene-2,6-diylidene)dimalononitrile (F6-TCNNQ), only ICT is found, illustrating the special behavior of PEN/F4-TCNQ at the border between CTC formation and ICT. We further study the photophysics of these donor/acceptor blends with respect to the importance of PEN as a SF material and find that SF is robust against moderate amounts of acceptors in the blends. Triplet pair formation and separation, as well as CT from PEN triplets to CTCs and acceptor molecules, is observed.



INTRODUCTION

Organic semiconductors attracted enormous attention due to their application in cost- and energy-efficient devices such as organic light-emitting diodes, transistors, and solar cells.¹ In the context of an optimized device performance, the transfer of charge in strongly interacting donor/acceptor systems is a key parameter for charge separation as well as for doping.^{2,3} Furthermore, in the last decade, the potential of multiexciton generation processes like singlet fission (SF) for the improvement of solar cell efficiency has been demonstrated.^{4–7} A model for the SF process with the evolution $S_0 + S_1 \rightarrow {}^1(TT) \rightarrow {}^1(T...T) \rightarrow T_1 + T_1$ has been established.⁵ Here, S_0 and S_1 denote singlet ground and lowest energy excited state, respectively, ${}^1(TT)$ is a triplet pair state with electronic coupling of the triplets, ${}^1(T...T)$ is a triplet pair state in which electronic coupling has been lost, and T_1 is the lowest energy triplet state.

To gain deeper insight into the microscopic mechanisms of both processes, charge-transfer (CT) and SF, pentacene (PEN) has been identified as a model system since it not only exhibits ultrafast and efficient SF^{8–12} but also finds wide application in organic transistors^{13,14} due to its high conductivity. Furthermore, PEN doped by 2,3,5,6-tetrafluoro-7,7,8,8-tetracyanoquinodimethane (F4-TCNQ) has been established as a prototypical system for the doping of organic semiconductors via charge-transfer complex (CTC) formation involving the hybridization of the frontier orbitals of dopant and host molecules¹⁵ in contrast to integer charge-transfer

(ICT).¹⁶ CTC formation has been successfully used to explain the relatively small doping efficiency in small-molecule organic semiconductors, and numerous examples of CTC formation since have been reported.^{17–22}

Recently, the model system of F4-TCNQ-doped PEN has been revisited from the theoretical perspective,³⁰ with the conclusion that it is at the boundary between CTC formation and ICT. To experimentally clarify the mechanisms of CT in this system, we investigated PEN/F4-TCNQ thin film blends with a wide range of mixing ratios and compared them to blends of PEN and 2,2'-(perfluoronaphthalene-2,6-diylidene)-dimalononitrile (F6-TCNNQ), which is a slightly stronger acceptor (see Figure 1). By expanding the spectral region of the absorption measurements down to 0.5 eV and performing additional vibrational measurements, we find evidence for both, ICT and CTC formation, in blends of PEN and F4-TCNQ, in agreement with the theoretical predictions³⁰ and a recent report of another donor/acceptor system.³¹ This is contrasted by blends of PEN and F6-TCNNQ that exhibit only ICT, illustrating the impact of slight changes in the acceptor strength and molecular size on the CT mechanism.

Received: August 23, 2021
Revised: October 7, 2021
Published: October 25, 2021



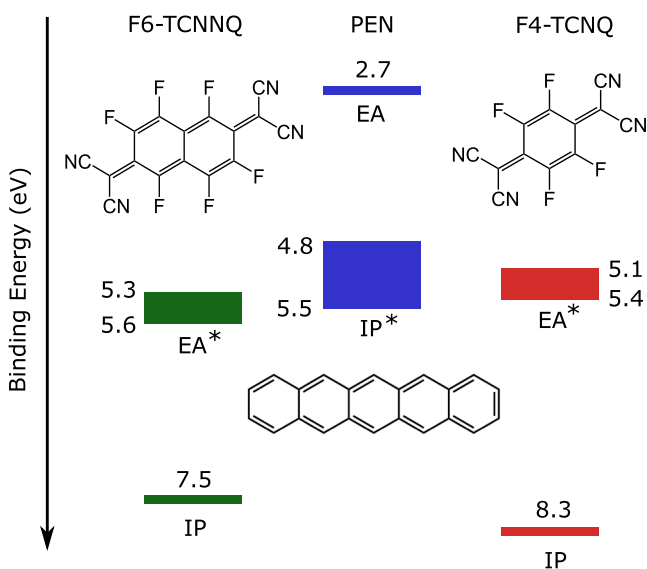


Figure 1. Molecular structures, electron affinities (EAs), and ionization potentials (IPs) of PEN, F4-TCNQ, and F6-TCNNQ.^{23–29} *For the EAs of the acceptors and the IP of PEN, an energy range is given, based on the reported values in the literature.^{23–28}

The PEN/F4-TCNQ and PEN/F6-TCNNQ blends are therefore prototypical systems to investigate the photophysical behavior of PEN in the presence of CTCs and ICT. Here, we use transient absorption (TA) spectroscopy in the visible and near-infrared (NIR) spectral regions to characterize the dynamics of photoinduced ion pair formation in equimolar

blends and to study the impact of donor/acceptor interactions on SF in blends with PEN excess.

EXPERIMENTAL METHODS

PEN and F4-TCNQ were purchased from Sigma-Aldrich with 99.995 and 99% purity and F6-TCNNQ from Novaled GmbH with 99.9% purity and used as received. Thin films were prepared by organic molecular beam deposition in a vacuum chamber with a base pressure of 2×10^{-8} mbar. The sample holder was cooled to ~ 253 K during the deposition of the thin films at a rate of 6 \AA min^{-1} and a nominal thickness of 80 nm. The growth rates of the two compounds of the blends were monitored independently by two quartz crystal microbalances, which were calibrated by ellipsometry and have an estimated error of $\pm 10\%$.

For steady-state absorption measurements, a PerkinElmer Lambda 950 UV–vis–NIR spectrometer was used. The X-ray reflectivity (XRR) measurements were performed on native silicon substrates on a General Electric XRD 3003TT instrument with Cu- $K_{\alpha 1}$ -radiation ($\lambda = 1.541 \text{ \AA}$). Grazing-incidence X-ray diffraction (GIXD) experiments were performed on a Xeuss 2.0, Xenocs laboratory instrument equipped with a microfocus X-ray source ($\lambda = 1.541 \text{ \AA}$) and a Pilatus 300k detector. Infrared spectra were measured in transmission mode on doubly polished, 1.5 mm thick silicon substrates using a Vertex 70 (Bruker) Fourier transform infrared (FTIR) spectrometer. Transient absorption (TA) measurements were performed using 150 μm thick borosilicate glass slides as substrates, which were sealed by a second glass in nitrogen to prevent photodegradation of the samples. The TA setup is a commercially available pump-probe setup (HELIOS, Ultrafast Systems). To generate the pump pulse, the

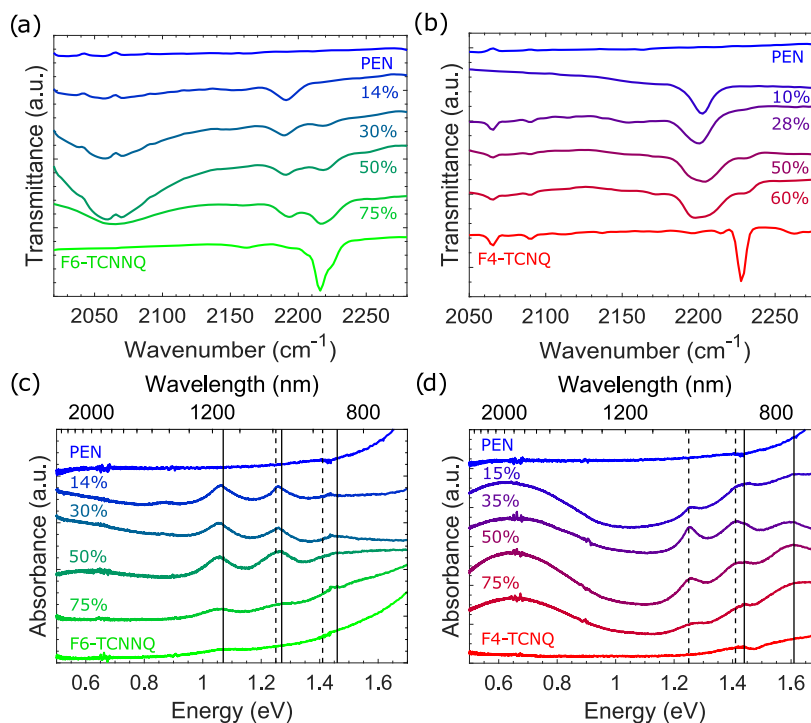


Figure 2. FTIR and NIR spectra of PEN/F6-TCNNQ (a, c) and PEN/F4-TCNQ (b, d) blends. The acceptor fractions are given in the figures, and the spectra are vertically offset for clarity. The vertical lines in the NIR spectra in (c) and (d) correspond to the reported cation and anion peak positions: The dashed lines are at the PEN cation peak positions, as reported in ref 34, the solid lines in (c) are at the F6-TCNNQ[−] anion peak positions reported in ref 25, and the solid lines in (d) are at the F4-TCNQ[−] anion peak position reported in ref 17.

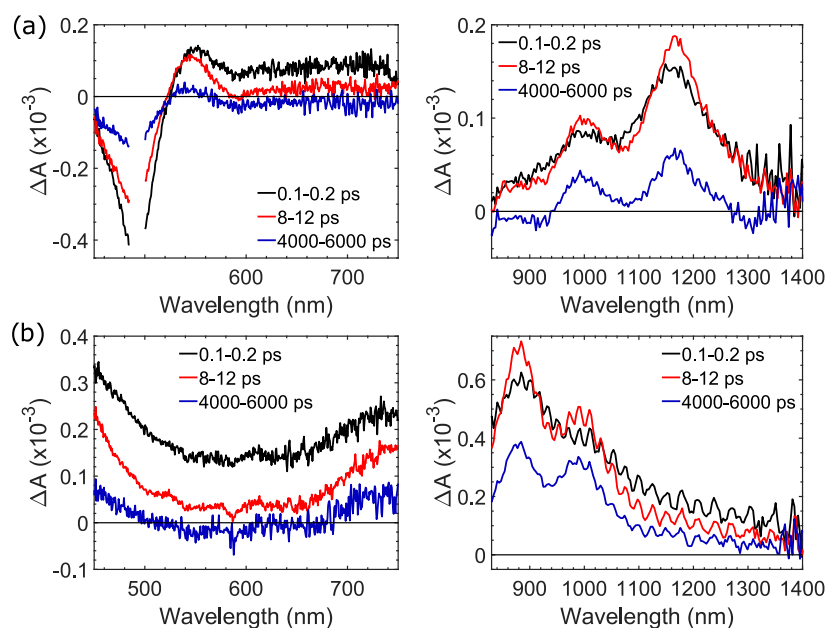


Figure 3. TA spectra integrated over the indicated pump-probe delay times of a blend with (a) 50% F6-TCNNQ pumped at 495 nm and (b) 50% F4-TCNQ pumped at 400 nm and probed in the visible (left) and NIR (right) spectral region. The oscillations in (b) in the NIR are measurement artifacts due to interference effects between the two sealed glasses.

fundamental beam at a center wavelength of 800 nm generated by a Ti:Sa amplified laser system (Astrella, Coherent, 4 kHz) was used as a pump in an optical parametric amplifier (TOPAS Prime, Light Conversion). White light supercontinuum generated in sapphire was used as probe; see ref 32 for details. All measurements were done with magic angle polarization between the pump and probe pulse. For global analysis (GA) of the obtained TA data, the open source software Glotaran³³ was used.

RESULTS

The structure of the thin films was investigated by XRR and GIXD measurements; see Figures S1 and S2 in the Supporting Information. These data lead to the conclusion of an amorphous mixed phase of PEN and the respective acceptor and, in blends with excess PEN, phase-separated, randomly oriented, polycrystalline PEN domains.

To characterize the degree of charge-transfer δ_{CT} in different blends, FTIR spectra were recorded, and the region of the CN stretching mode, shown in Figure 2a,b, was analyzed. PEN does not show any vibrational signal in this region which allows us to assign all features to the respective acceptor. For neat F6-TCNNQ, a relatively strong signal is obtained with peaks at 2223, 2216, and 2207 cm^{-1} , with the strongest one at 2216 cm^{-1} as reported before.^{19,26,31} For increasing fractions of PEN in the blends, this signal continuously decreases in intensity. Simultaneously, a signal around 2191 cm^{-1} appears that can be assigned to the CN stretching mode of F6-TCNNQ⁻ anions,^{26,31} dominating for the 14% F6-TCNNQ blend. The additional broad peak around 2065 cm^{-1} , observed for the blends, is tentatively assigned to interactions between the charges in the organic thin films and oxygen vacancies in SiO_2 due to its width.³⁵ In summary, the data allow the conclusion that in the blends, both, neutral and ionized F6-TCNNQ molecules are present. This scenario is supported by the NIR absorption spectra in Figure 2c as the sharp peaks at 1.06 eV (1170 nm), 1.26 eV (985 nm), and 1.45 eV (855 nm)

match the positions reported for the F6-TCNNQ⁻ anion^{25,36} and PEN⁺ cation absorption.³⁴ We note here that the weak absorption below 0.7 eV in the spectra of the blends with 14 and 30% F6-TCNNQ might indicate a small fraction of CTCs with a large δ_{CT} . However, we conclude from the strong F6-TCNNQ⁻ anion and PEN⁺ cation peaks that ICT is the dominant mechanism.

For the blends with F4-TCNQ, a different picture is obtained based on the shift of the CN stretching mode (Figure 2b). Neat F4-TCNQ shows one main sharp peak at 2228 cm^{-1} in accordance with the literature.¹⁷ Upon addition of PEN, three peaks can be discerned: At 2230 cm^{-1} , a weak peak, assigned to neutral F4-TCNQ, is observable, which decreases in intensity with increasing PEN fraction. At 2193 cm^{-1} , a peak is visible that becomes less intense for increasing PEN fraction and is assigned to F4-TCNQ⁻ anions based on the literature,^{17,37} indicating ICT. Finally, there is a peak at 2203 cm^{-1} , which is visible in all blends and dominates in the blend with 10% F4-TCNQ. Due to its intermediate position between the ionic and neutral F4-TCNQ CN stretching mode, this peak is assigned to a CTC formed by PEN and F4-TCNQ with $\delta_{CT} = (0.72 \pm 0.05)e$ (ref 14, 17). This indicates the coexistence of ICT and CTC formation in blends of PEN and F4-TCNQ as observed before in a related system (dibenzotetrathiafulvalene/F6-TCNNQ)³¹ and consistent with the NIR absorption spectra (Figure 2d). Here, the spectra of the blends also show sharp peaks at 1.26 eV (985 nm), 1.42 eV (875 nm), 1.44 eV (860 nm), and 1.60 eV (775 nm) that match the absorption of F4-TCNQ⁻ anions^{17,38} and PEN⁺ cations.³⁴ However, there is an additional broad absorption peak at even lower energies, around 0.65 eV (1910 nm), that we ascribe to electronic transitions of a CTC, based on the broad shape and the low energy position.^{17,39}

The comparison of PEN blends with F6-TCNNQ and F4-TCNQ, respectively, allows us to investigate the photophysics of donor/acceptor blends at the boundary between ICT and CTC formation using ultrafast TA spectroscopy. For reference,

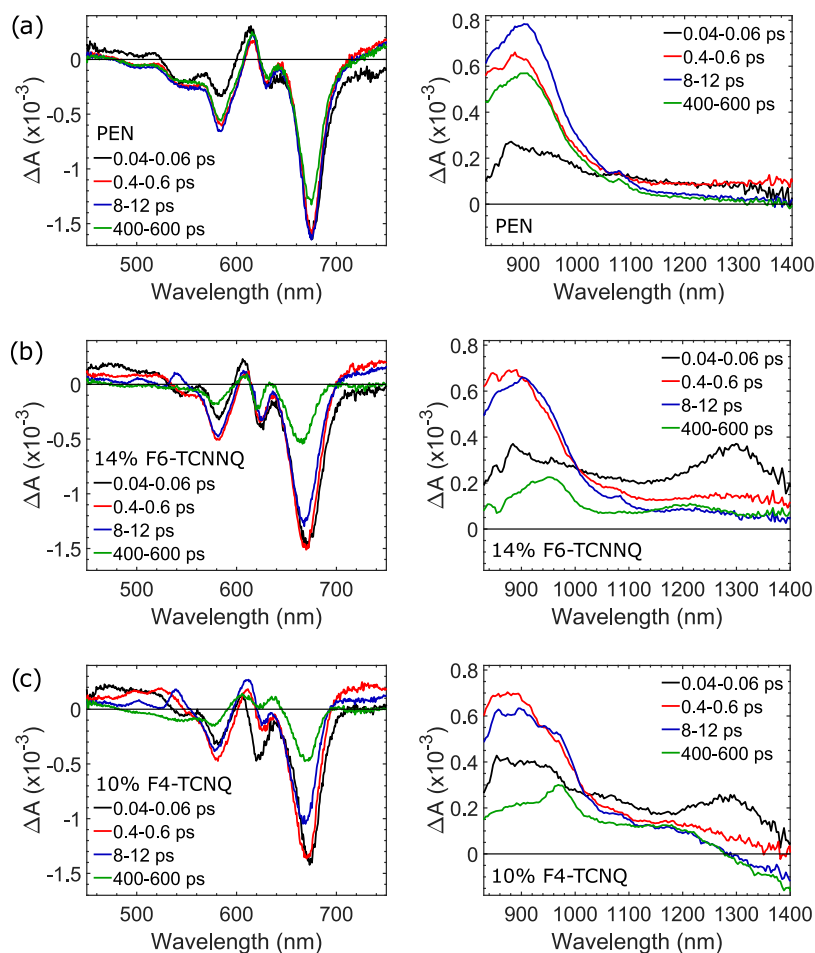


Figure 4. TA spectra integrated over the indicated pump-probe delay times of (a) PEN, (b) 14% F6-TCNNQ, and (c) 10% F4-TCNQ pumped at 620 nm and probed in the visible (left) and NIR (right) spectral region.

steady-state absorption spectra of the investigated blends are shown in the Supporting Information, Figure S3. In Figure 3a, TA spectra of a blend with 50% F6-TCNNQ pumped at 495 nm and probed in the visible and NIR spectral regions are shown, which display only minor spectral evolution and a slow, nonexponential decay. The TA spectra in the visible exhibit a ground-state bleach (GSB) at an absorption maximum of 495 nm and a feature related to the Stark effect⁴⁰ around 545 nm. The NIR TA spectra show pronounced photoinduced absorption (PIA) peaked at 1170 and 1000 nm and a shoulder around 880 nm, thus at the positions of the F6-TCNNQ⁻ anion and PEN⁺ cation absorption^{25,34} (see Figure 2c). These signals would be consistent with optical excitation of neutral F6-TCNNQ molecules by the pump pulse followed by F6-TCNNQ⁻ anion and PEN⁺ cation formation via the transfer of an electron from PEN to F6-TCNNQ. In the visible TA spectra of the blend with 50% F4-TCNQ pumped at 400 nm (Figure 3b), PIAs peaked outside our measurement region and, in the NIR TA spectra, PIAs peaked at 880 and 990 nm are observed at the positions of the F4-TCNQ⁻ anion and PEN⁺ cation absorption^{17,34} (Figure 2d), supporting the notion of a similar scenario as for the F6-TCNNQ blend.

The steady-state absorption spectra of the blends with excess PEN show characteristic PEN features (Figure S3 in the Supporting Information) and therefore allow a comparison to a neat PEN film. The TA spectra of a neat PEN film pumped at 620 nm and probed in the visible and NIR region are shown in

Figure 4a. From GA of the data in the visible spectral region (see the Supporting Information), a time constant of $\tau_1 = 95 \left(\begin{smallmatrix} +20 \\ -7 \end{smallmatrix} \right)$ fs was extracted for the $S_1 \rightarrow {}^1(TT)$ evolution, based on the loss of stimulated emission (SE) and appearance of triplet excited-state absorption (ESA) above 700 nm, in very good agreement with the literature.^{11,41} The further evolution into ${}^1(T...T)$ cannot be monitored in the visible region in neat thin film PEN under perpendicular illumination due to the absence of strong triplet features.¹⁰ However, in the NIR region, a spectral difference was reported for the ${}^1(TT)$ and ${}^1(T...T)$ species,^{8,42} which is also found in our data as a shift of the main ESA toward slightly larger wavelengths and loss of ESA above 1100 nm, even at room temperature. From GA (see the Supporting Information), a time constant of $\tau_2 = 1.29 \left(\begin{smallmatrix} +0.13 \\ -0.12 \end{smallmatrix} \right)$ ps was found for the ${}^1(TT) \rightarrow {}^1(T...T)$ transition, consistent with earlier reports.^{10,42}

In Figure 4b,c, the TA spectra of the blend with 14% F6-TCNNQ and the blend with 10% F4-TCNQ are shown. The TA spectra of the blends with 30% F6-TCNNQ and 28% F4-TCNQ can be found in the Supporting Information in Figure S5 and two-dimensional (2D) map representations of all films in Figures S6 and S7. The incorporation of acceptor molecules into the PEN thin film not only impacts the photophysics due to their strong electron-accepting behavior but also affects the PEN crystallite orientation, seen in the structural analysis. This,

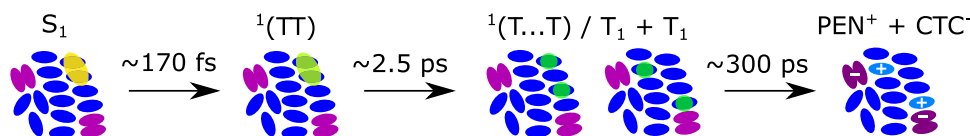


Figure 5. Schematic representation of the involved photoinduced species in PEN/F4-TCNQ blends with PEN excess. Blue ellipsoids represent PEN molecules, CTCs are depicted in purple, singlet excitons in yellow, and triplet excitons in green. ${}^1(T\dots T)$ and $T_1 + T_1$ show no spectroscopic difference and the last step is diffusion-driven; therefore, only an approximate T_1 decay time is given. Reverse processes and decay to the ground state are omitted for clarity. For the PEN/F6-TCNNQ blends, the last step is CT to F6-TCNNQ or F6-TCNNQ $^-$.

in turn, modifies the visibility of PEN transitions in the TA spectrum.^{10,12,43} Both effects can be seen in the TA spectra shown in Figure 4b,c. In the visible region of the spectra, the appearance of sharp ESA peaks at 500 and 540 nm can be explained by a change of the PEN crystallite orientation, making PEN triplet transitions at these positions excitable with our measurement geometry.¹² These ESA features are evolving and slightly shifting within the first picoseconds, which can be ascribed to the evolution from ${}^1(TT)$ to ${}^1(T\dots T)$ (see ref 42), and which again can also be followed in the NIR spectra.⁸ A second orientation effect can be seen in the NIR spectra as an ESA around 1300 nm at very short times, which we ascribe to the singlet TA spectrum based on ref 42.

The impact of acceptor molecules on the PEN photophysics can be followed in the visible and NIR TA spectra on longer time scales. While neat PEN does not show any spectral evolution after 10 ps, the shape of the spectra of the blends changes on these time scales. The PEN triplet ESA in the visible spectral region (at 540 nm and above 700 nm) decays within 500 ps, while the PEN GSB remains. In the NIR TA spectra of the PEN/F6-TCNNQ blend in Figure 4b, a PIA between 850 and 1000 nm and a weaker PIA around 1200 nm rise at long delay times, thus at the positions of the PEN $^+$ cation and F6-TCNNQ $^-$ anion absorption shown in Figure 2c. The NIR spectra in Figure 4c show at long times PIAs at the positions of the PEN $^+$ cation and F4-TCNQ $^-$ anion absorption (compare Figure 2d) and a bleach above 1300 nm that matches the CTC transition.

DISCUSSION

Summarizing our experimental findings, we provide conclusive evidence for the coexistence of CTC formation and ICT in blends of PEN and F4-TCNQ, confirming theoretical predictions that F4-TCNQ-doped PEN is at the boundary between CTC formation and ICT.³⁰ This was achieved by expanding the measured spectral region of the absorption spectra down to 0.5 eV and comparing these results with FTIR spectra, allowing us to observe signatures of both CT mechanisms. In particular, the high sensitivity of the CTC formation on long-range order³¹ is confirmed in our experiments. We find that CTC formation dominates in PEN/F4-TCNQ blends with an excess of PEN for which Bragg peaks indicate pronounced long-range order. In contrast, it seems that ICT is more likely for those mixing ratios for which the molecular arrangement is less ordered and the probability of defects is increased. A possible explanation is that increased disorder facilitates a variation of the relative arrangement of donor and acceptor molecules and thus reduced orbital overlap. By comparing these results to blends of PEN with the slightly stronger acceptor F6-TCNNQ, the special case of PEN/F4-TCNQ blends becomes apparent as the small differences in the acceptor strength and molecular size are already sufficient to push the system across the boundary

toward preferential ICT independent of the mixing ratio and the resulting long-range order.

Interestingly, independent of the acceptor used, the photophysics of equimolar blends is dominated by the decay of ion pairs resulting from CT between PEN and the excited acceptor. This can be explained by a dominant excitation of neutral acceptor molecules in both blends (compare their solution absorption spectra²⁵) and subsequent CT. We thus turn to the discussion of blends with an excess of PEN, in which the PEN excess molecules in phase-separated domains can directly be excited using an excitation wavelength of 620 nm (see the Supporting Information). Based on the previously described observations and performing GA (see the Supporting Information) of the TA data in the visible and the NIR of the blends with 10% (14%) and 28% (30%) F4-TCNQ (F6-TCNNQ), we propose the kinetic scheme shown in Figure 5 to describe the photophysics of these blends.

The 620 nm pump pulse excites singlets on PEN molecules (S_1) that undergo an ultrafast transition to an electronically coupled ${}^1(TT)$ state with a time constant τ_1 between 110 and 230 fs, slightly slower than in the neat PEN film. It follows a transition with a time constant τ_2 between 1.8 and 3.3 ps to a ${}^1(T\dots T)$ state, again slightly slower than in neat PEN. These similar time constants suggest that PEN undergoes coherent SF also in the presence of some acceptor molecules in the film, which do not significantly impact this process. In particular, we have no indications for a mediating role of the CT between PEN and the electron acceptor in the SF process in our blends. The further evolution differs for the two different acceptors. In the blends with F4-TCNQ, the long-lived bleach of the energetically low CTC transition combined with the PIA of PEN $^+$ cations suggests an electron transfer from a PEN triplet to a CTC, resulting in additional PEN $^+$ cations and negatively charged CTCs. Since this evolution is driven by the diffusion of excitons and depends on the distance of the created PEN triplet to the CTCs, it has a nonexponential behavior. Consequently, only a rough estimate of ~ 300 ps can be given, based on the time scale of the quenching of the triplet ESA (see Figure S8 in the Supporting Information). In the blends containing F6-TCNNQ, the triplet ESA of PEN is also quenched much faster than in neat PEN, although CTC formation is not observed. The remaining of the GSB and the build-up of PEN $^+$ cation PIA accompanied by a weaker PIA at the position of F6-TCNNQ $^-$ anion absorption could be explained by a combination of the following two effects. First, CT of an electron from a PEN triplet to neutral F6-TCNNQ, leading to PEN $^+$ cations and F6-TCNNQ $^-$ anions, and possibly second, a CT from PEN triplets to F6-TCNNQ $^-$ anions, resulting in PEN $^+$ cations and F6-TCNNQ $^{2-}$ dianions. The formation of F6-TCNNQ $^{2-}$ dianions has been reported before in the context of double doping,³⁸ but these dianions do not show any absorption in our accessible spectral region⁴⁴ so that their formation cannot be proven. However, the scenario

would be consistent with the FTIR spectra in Figure 2c, which indicate that a large fraction of the F6-TCNNQ molecules in these blends is already ionized in the ground state. Similar to the blends with F4-TCNNQ, the process of triplet quenching is probably diffusion-driven, which explains the nonexponential behavior and the similar time of ~ 300 ps until the triplet signal has disappeared. Finally, the weaker PEN GSB signal in all blends after 500 ps compared to neat PEN implies that a fraction of the PEN triplets in the blends directly decays back to the ground state, probably accelerated by smaller crystallite sizes in the blends or energy transfer to CTCs.

CONCLUSIONS

In summary, we have revisited the CT interactions of PEN and F4-TCNNQ in thin film blends to unify the existing models for CT in this system.^{15,16,30} Clear evidence is found for a coexistence of CTC formation as well as ICT, with the relative contribution depending on the mixing ratio. While at relatively small F4-TCNNQ fractions CTC formation is facilitated, ICT becomes more and more important with increasing F4-TCNNQ fraction in the blends, possibly due to reduced long-range order. Blends of PEN and F6-TCNNQ, on the other hand, show only ICT, which can be rationalized by the slightly higher electron affinity of F6-TCNNQ compared to F4-TCNNQ. This underlines the sensitivity of the CT mechanism to changes in the acceptor strength, as a slight increase seems to be sufficient to suppress CTC formation.

The dynamics of the equimolar blends are dominated by the formation and decay of ion pairs, whereas the major decay channel in blends with excess of PEN is SF. Importantly, despite the presence of strong acceptors, the PEN triplet pair formation is only slightly slowed down in comparison to neat PEN and still occurs within a few 100 fs. On longer time scales, CT from PEN triplets to CTCs and acceptor molecules is observed, which results in long-lived charged molecules in the blends. Our findings clarify the open question of the CT mechanism in the model system PEN/F4-TCNNQ and emphasize its special status at the boundary between the two main mechanisms, CTC formation and ICT. In addition, the results of ultrafast spectroscopy experiments suggest that SF is a very robust process in PEN, even in the presence of considerable amounts of strong electron acceptors.

ASSOCIATED CONTENT

Supporting Information

The Supporting Information is available free of charge at <https://pubs.acs.org/doi/10.1021/acs.jpcc.1c07457>.

Additional experimental data and discussions: X-ray diffraction data, additional steady-state absorption spectra, transient absorption data, and details of global analysis (PDF)

AUTHOR INFORMATION

Corresponding Authors

Petra Tegeder – *Physikalisch-Chemisches Institut, Universität Heidelberg, 69120 Heidelberg, Germany; Centre for Advanced Materials, Universität Heidelberg, 69120 Heidelberg, Germany*; orcid.org/0000-0002-5071-9385; Email: tegeder@uni-heidelberg.de

Katharina Broch – *Institut für Angewandte Physik, Universität Tübingen, 72076 Tübingen, Germany; Center for Light-Matter Interactions, Sensors & Analytics (LISA⁺)*

Universität Tübingen, 72076 Tübingen, Germany;
orcid.org/0000-0002-9354-292X; Email: katharina-anna.broch@uni-tuebingen.de

Authors

Christoph P. Theurer – *Institut für Angewandte Physik, Universität Tübingen, 72076 Tübingen, Germany*

Martin Richter – *Physikalisch-Chemisches Institut, Universität Heidelberg, 69120 Heidelberg, Germany*

Debkumar Rana – *Physikalisch-Chemisches Institut, Universität Heidelberg, 69120 Heidelberg, Germany; Centre for Advanced Materials, Universität Heidelberg, 69120 Heidelberg, Germany*

Giuliano Duva – *Institut für Angewandte Physik, Universität Tübingen, 72076 Tübingen, Germany*; Present Address: NMI Naturwissenschaftliches und Medizinisches Institut an der Universität Tübingen Markwiesenstraße 55, 72770 Reutlingen, Germany; orcid.org/0000-0001-9492-3276

Daniel Lepple – *Institut für Angewandte Physik, Universität Tübingen, 72076 Tübingen, Germany*

Alexander Hinderhofer – *Institut für Angewandte Physik, Universität Tübingen, 72076 Tübingen, Germany*; orcid.org/0000-0001-8152-6386

Frank Schreiber – *Institut für Angewandte Physik, Universität Tübingen, 72076 Tübingen, Germany; Center for Light-Matter Interactions, Sensors & Analytics (LISA⁺), Universität Tübingen, 72076 Tübingen, Germany*; orcid.org/0000-0003-3659-6718

Complete contact information is available at:

<https://pubs.acs.org/doi/10.1021/acs.jpcc.1c07457>

Notes

The authors declare no competing financial interest.

ACKNOWLEDGMENTS

The authors acknowledge funding by the German Research Foundation (DFG) through the projects TE479/6-1, BR4869/4-1, and SCHR700/40-1. M.R. acknowledges financial support from the Heidelberg Graduate School of Fundamental Physics. D.R. acknowledges funding by the Max Planck School Matter To Life project. G.D. gratefully acknowledges support from the Carl-Zeiss-Stiftung.

REFERENCES

- (1) Forrest, S. R. The Path to Ubiquitous and Low-Cost Organic Electronic Appliances on Plastic. *Nature* **2004**, *428*, 911–918.
- (2) Salzmann, I.; Heimel, G. Toward a Comprehensive Understanding of Molecular Doping Organic Semiconductors (Review). *J. Electron Spectrosc. Relat. Phenom.* **2015**, *204*, 208–222.
- (3) Vandewal, K. Interfacial Charge Transfer States in Condensed Phase Systems. *Annu. Rev. Phys. Chem.* **2016**, *67*, 113–133.
- (4) Smith, M. B.; Michl, J. Singlet Fission. *Chem. Rev.* **2010**, *110*, 6891–6936.
- (5) Miyata, K.; Conrad-Burton, F. S.; Geyer, F. L.; Zhu, X.-Y. Triplet Pair States in Singlet Fission. *Chem. Rev.* **2019**, *119*, 4261–4292.
- (6) Gish, M. K.; Pace, N. A.; Rumbles, G.; Johnson, J. C. Emerging Design Principles for Enhanced Solar Energy Utilization with Singlet Fission. *J. Phys. Chem. C* **2019**, *123*, 3923–3934.
- (7) Wilson, M. W. B.; Rao, A.; Ehrler, B.; Friend, R. H. Singlet Exciton Fission in Polycrystalline Pentacene: From Photophysics Toward Devices. *Acc. Chem. Res.* **2013**, *46*, 1330–1338.
- (8) Yong, C. K.; Musser, A. J.; Bayliss, S. L.; Lukman, S.; Tamura, H.; Bubnova, O.; Hallani, R. K.; Meneau, A.; Resel, R.; Maruyama,

M.; et al. The Entangled Triplet Pair State in Acene and Heteroacene Materials. *Nat. Commun.* **2017**, *8*, No. 15953.

(9) Congreve, D. N.; Lee, J.; Thompson, N. J.; Hontz, E.; Yost, S. R.; Reuswig, P. D.; Bahlke, M. E.; Reineke, S.; Van Voorhis, T.; Baldo, M. A. External Quantum Efficiency Above 100% in a Singlet-Exciton-Fission-Based Organic Photovoltaic Cell. *Science* **2013**, *340*, 334–337.

(10) Marciniak, H.; Pugliesi, I.; Nickel, B.; Lochbrunner, S. Ultrafast Singlet and Triplet Dynamics in Microcrystalline Pentacene Films. *Phys. Rev. B* **2009**, *79*, No. 235318.

(11) Wilson, M. W.; Rao, A.; Clark, J.; Kumar, R. S. S.; Brida, D.; Cerullo, G.; Friend, R. H. Ultrafast Dynamics of Exciton Fission in Polycrystalline Pentacene. *J. Am. Chem. Soc.* **2011**, *133*, 11830–11833.

(12) Rao, A.; Wilson, M. W. B.; Albert-Seifried, S.; Di Pietro, R.; Friend, R. H. Photophysics of Pentacene Thin Films: The Role of Exciton Fission and Heating Effects. *Phys. Rev. B* **2011**, *84*, No. 195411.

(13) Gershenson, M. E.; Podzorov, V.; Morpurgo, A. F. Colloquium: Electronic Transport in Single-Crystal Organic Transistors. *Rev. Mod. Phys.* **2006**, *78*, 973–989.

(14) Harada, K.; Sumino, M.; Adachi, C.; Tanaka, S.; Miyazaki, K. Improved Thermoelectric Performance of Organic Thin-Film Elements Utilizing a Bilayer Structure of Pentacene and 2, 3, 5, 6-tetrafluoro-7, 7, 8, 8-tetracyanoquinodimethane (F4-TCNQ). *Appl. Phys. Lett.* **2010**, *96*, No. 253304.

(15) Salzmann, I.; Heimel, G.; Duhm, S.; Oehzelt, M.; Pingel, P.; George, B. M.; Schnegg, A.; Lips, K.; Blum, R.-P.; Vollmer, A.; et al. Intermolecular Hybridization Governs Molecular Electrical Doping. *Phys. Rev. Lett.* **2012**, *108*, No. 035502.

(16) Ha, S. D.; Kahn, A. Isolated Molecular Dopants in Pentacene Observed by Scanning Tunneling Microscopy. *Phys. Rev. B* **2009**, *80*, No. 195410.

(17) Méndez, H.; Heimel, G.; Winkler, S.; Frisch, J.; Opitz, A.; Sauer, K.; Wegner, B.; Oehzelt, M.; Röthel, C.; Duhm, S.; et al. Charge-Transfer Crystallites as Molecular Electrical Dopants. *Nat. Commun.* **2015**, *6*, No. 8560.

(18) Salzmann, I.; Heimel, G.; Oehzelt, M.; Winkler, S.; Koch, N. Molecular Electrical Doping of Organic Semiconductors: Fundamental Mechanisms and Emerging Dopant Design Rules. *Acc. Chem. Res.* **2016**, *49*, 370–378.

(19) Duva, G.; Beyer, P.; Scholz, R.; Belova, V.; Opitz, A.; Hinderhofer, A.; Gerlach, A.; Schreiber, F. Ground-State Charge-Transfer Interactions in Donor:Acceptor Pairs of Organic Semiconductors—a Spectroscopic Study of Two Representative Systems. *Phys. Chem. Chem. Phys.* **2019**, *21*, 17190–17199.

(20) Belova, V.; Beyer, P.; Meister, E.; Linderl, T.; Halbich, M.-U.; Gerhard, M.; Schmidt, S.; Zechel, T.; Meisel, T.; Generalov, A. V.; et al. Evidence for Anisotropic Electronic Coupling of Charge Transfer States in Weakly Interacting Organic Semiconductor Mixtures. *J. Am. Chem. Soc.* **2017**, *139*, 8474–8486.

(21) Hinderhofer, A.; Schreiber, F. Organic–Organic Heterostructures: Concepts and Applications. *Chem. Phys. Chem.* **2012**, *13*, 628–643.

(22) Schwarze, M.; Schellhammer, K. S.; Ortstein, K.; Benduhn, J.; Gaul, C.; Hinderhofer, A.; Toro, L. P.; Scholz, R.; Kublitski, J.; Roland, S.; et al. Impact of Molecular Quadrupole Moments on the Energy Levels at Organic Heterojunctions. *Nat. Commun.* **2019**, *10*, No. 2466.

(23) Yoshida, H.; Yamada, K.; Tsutsumi, J.; Sato, N. Complete Description of Ionization Energy and Electron Affinity in Organic Solids: Determining Contributions from Electronic Polarization, Energy Band Dispersion, and Molecular Orientation. *Phys. Rev. B* **2015**, *92*, No. 075145.

(24) Kanai, K.; Akaike, K.; Koyasu, K.; Sakai, K.; Nishi, T.; Kamizuru, Y.; Nishi, T.; Ouchi, Y.; Seki, K. Determination of Electron Affinity of Electron Accepting Molecules. *Appl. Phys. A* **2009**, *95*, 309–313.

(25) Koech, P. K.; Padmaperuma, A. B.; Wang, L.; Swensen, J. S.; Polikarpov, E.; Darsell, J. T.; Rainbolt, J. E.; Gaspar, D. J. Synthesis

and Application of 1, 3, 4, 5, 7, 8-Hexafluorotetracyanoquinodimethane (F6-TNAP): A Conductivity Dopant for Organic Light-Emitting Devices. *Chem. Mater.* **2010**, *22*, 3926–3932.

(26) Karpov, Y.; Erdmann, T.; Stamm, M.; Lappan, U.; Guskova, O.; Malanin, M.; Raguzin, I.; Beryozkina, T.; Bakulev, V.; Günther, F.; et al. Molecular Doping of a High Mobility Diketopyrrolopyrrole-Dithienylthieno [3, 2-b] thiophene Donor-Acceptor Copolymer with F6TCNNQ. *Macromolecules* **2017**, *50*, 914–926.

(27) Zhang, F.; Kahn, A. Investigation of the High Electron Affinity Molecular Dopant F6-TCNNQ for Hole-Transport Materials. *Adv. Funct. Mater.* **2018**, *28*, No. 1703780.

(28) Gao, W.; Kahn, A. Controlled p-Doping of Zinc Phthalocyanine by Coevaporation with Tetrafluorotetracyanoquinodimethane: A Direct and Inverse Photoemission Study. *Appl. Phys. Lett.* **2001**, *79*, 4040–4042.

(29) Gerbert, D.; Maaß, F.; Tegeder, P. Extended Space Charge Region and Unoccupied Molecular Band Formation in Epitaxial Tetrafluorotetracyanoquinodimethane Films. *J. Phys. Chem. C* **2017**, *121*, 15696–15701.

(30) Li, J.; D'Avino, G.; Pershin, A.; Jacquemin, D.; Duchemin, I.; Beljonne, D.; Blase, X. Correlated Electron-Hole Mechanism for Molecular Doping in Organic Semiconductors. *Phys. Rev. Mater.* **2017**, *1*, No. 025602.

(31) Beyer, P.; Pham, D.; Peter, C.; Koch, N.; Meister, E.; Brütting, W.; Grubert, L.; Hecht, S.; Nabok, D.; Cocchi, C.; et al. State-of-Matter-Dependent Charge-Transfer Interactions Between Planar Molecules for Doping Applications. *Chem. Mater.* **2019**, *31*, 1237–1249.

(32) Alagna, N.; Lustres, J. L. P.; Roozbeh, A.; Han, J.; Hahn, S.; Berger, F. J.; Zaumseil, J.; Dreuw, A.; Bunz, U. H.; Buckup, T. Ultrafast Singlet Fission in Rigid Azaarene Dimers with Negligible Orbital Overlap. *J. Phys. Chem. B* **2020**, *124*, 9163–9174.

(33) Snellenburg, J. J.; Laptinok, S. P.; Seger, R.; Mullen, K. M.; van Stokkum, I. H. M. Glotaran: A Java-Based Graphical User Interface for the R-Package TIMP. *J. Stat. Software* **2012**, *49*, 1–22.

(34) Brinkmann, M.; Videva, V. S.; Bieber, A.; André, J. J.; Turek, P.; Zuppiroli, L.; Bugnon, P.; Schaer, M.; Nuesch, F.; Humphry-Baker, R. Electronic and Structural Evidences for Charge Transfer and Localization in Iodine-Doped Pentacene. *J. Phys. Chem. A* **2004**, *108*, 8170–8179.

(35) Lu, Z.-Y.; Nicklaw, C. J.; Fleetwood, D. M.; Schrimpf, R. D.; Pantelides, S. T. Structure, Properties, and Dynamics of Oxygen Vacancies in Amorphous SiO₂. *Phys. Rev. Lett.* **2002**, *89*, No. 285505.

(36) Isenberg, C.; Saragi, T. P. Revealing the Origin of Magnetoresistance in Unipolar Amorphous Organic Field-Effect Transistors. *J. Mater. Chem. C* **2014**, *2*, 8569–8577.

(37) Meneghetti, M.; Pecile, C. Charge-Transfer Organic Crystals: Molecular Vibrations and Spectroscopic Effects of Electron-Molecular Vibration Coupling of the Strong Electron Acceptor TCNQF₄. *J. Chem. Phys.* **1986**, *84*, 4149–4162.

(38) Kiefer, D.; Kroon, R.; Hofmann, A. I.; Sun, H.; Liu, X.; Giovannitti, A.; Stegerer, D.; Cano, A.; Hynynen, J.; Yu, L.; et al. Double Doping of Conjugated Polymers with Monomer Molecular Dopants. *Nat. Mater.* **2019**, *18*, 149–155.

(39) Theurer, C. P.; Valencia, A. M.; Hausch, J.; Zeiser, C.; Sivanesan, V.; Cocchi, C.; Tegeder, P.; Broch, K. Photophysics of Charge Transfer Complexes Formed by Tetracene and Strong Acceptors. *J. Phys. Chem. C* **2021**, *125*, 6313–6323.

(40) Ishino, Y.; Miyata, K.; Sugimoto, T.; Watanabe, K.; Matsumoto, Y.; Uemura, T.; Takeya, J. Ultrafast Exciton Dynamics in Dinaphtho [2,3-b:2'3'-f] thieno [3,2-b]-thiophene Thin Films. *Phys. Chem. Chem. Phys.* **2014**, *16*, 7501–7512.

(41) Bakulin, A. A.; Morgan, S. E.; Kehoe, T. B.; Wilson, M. W.; Chin, A. W.; Zigmantas, D.; Egorova, D.; Rao, A. Real-Time Observation of Multiexcitonic States in Ultrafast Singlet Fission Using Coherent 2D Electronic Spectroscopy. *Nat. Chem.* **2016**, *8*, 16–23.

(42) Pensack, R. D.; Ostroumov, E. E.; Tilley, A. J.; Mazza, S.; Grieco, C.; Thorley, K. J.; Asbury, J. B.; Seferos, D. S.; Anthony, J. E.;

Scholes, G. D. Observation of Two Triplet-Pair Intermediates in Singlet Exciton Fission. *J. Phys. Chem. Lett.* **2016**, *7*, 2370–2375.

(43) Khan, S.; Mazumdar, S. Theory of Transient Excited State Absorptions in Pentacene and Derivatives: Triplet-Triplet Biexciton versus Free Triplets. *J. Phys. Chem. Lett.* **2017**, *8*, 5943–5948.

(44) Meisel, T.; Sparenberg, M.; Gawek, M.; Sadofev, S.; Kobin, B.; Grubert, L.; Hecht, S.; List-Kratochvil, E.; Blumstengel, S. Fingerprint of Charge Redistribution in the Optical Spectra of Hybrid Inorganic/Organic Semiconductor Interfaces. *J. Phys. Chem. C* **2018**, *122*, 12913–12919.